A&A 468, 563–569 (2007)
DOI: 10.1051/0004-6361:20066219

Astronomy & Astrophysics

A model of the light curves of gamma-ray bursts

W. H. Lei, D. X. Wang, B. P. Gong, and C. Y. Huang

Department of Physics, Huazhong University of Science and Technology, Wuhan, 430074, P.R. China
e-mail: dxwang@mail.hust.edu.cn

Received 9 August 2006 / Accepted 6 March 2007

ABSTRACT

Aims. An extreme Kerr black hole (BH) surrounded by a precessing disk is invoked to explain the light curves of gamma-ray bursts (GRBs) based on the coexistence of the Blandford-Znajek (BZ) and the magnetic coupling (MC) processes.
Methods. The overall shape of the light curves and the duration of GRBs are interpreted by the evolution of the half-opening angle of the magnetic flux on the BH horizon, and the complex temporal structures are modulated by the precession and nutation of the jet powered by the BZ process.
Results. The time profile of the emission exhibits a fast rise and a slow decay due to the effect of the evolution of the half-opening angle. The light curves of several GRBs are well fitted by this model with only six free parameters.

Key words. gamma rays: bursts – black hole physics – accretion, accretion disk – magnetic fields

1. Introduction

Gamma ray bursts (GRBs) are possibly the most luminous objects in the Universe. Extremely high energy released in very short timescales suggests that GRBs involve the formation of a black hole (BH) via a catastrophic stellar collapse event or possibly a neutron star merger, implying that an inner engine could be built on an accreting BH (Piran 2004).

Among a variety of mechanisms for powering GRBs, the BZ process (Blandford & Znajek 1977) has the unique advantage of providing "clean" (free of baryonic contamination) energy by extracting rotating energy from a BH and transferring it in the form of Poynting flow in the outgoing energy flux (Lee et al. 2000). Recently, observations and theoretical considerations have linked long-duration GRBs with ultrabright Type Ib/c SNe (Galama et al. 1998; Bloom et al. 1999). Brown et al. (2000) proposed a specific scenario for a GRB-SN connection. They argued that the GRB is powered by the BZ process and the SN is powered by the MC process, which is regarded as one of the variants of the BZ process (van Putten 1999; Blandford 1999; Li 2000, 2002; Wang et al. 2002). However, they failed to distinguish the fractions of the energy for these two objects. More recently, van Putten and collaborators proposed a dominant spin-connection between the central BH and surrounding high-density matter (van Putten 2001; van Putten & Levinson 2003). It is based on similar shapes in topology of the torus magnetosphere with the magnetosphere of pulsars, when viewed in a poloidal cross-section. This description points towards complete calorimetry on GRB-SNe, upon including an unexpectedly powerful long-duration burst of gravitational-radiation, representing most of the spin-energy liberated from the central BH.

Lei et al. (2005, hereafter LWM05) proposed a scenario for GRBs in Type Ib/c SNe, invoking the coexistence of the BZ and MC processes. In LWM05 the half-opening angle of the magnetic flux tube on the horizon is determined by the mapping relation between the angular coordinate on the BH horizon and the radial coordinate on the surrounding accretion disk. In this scenario the half-opening angle evolves to zero with the spinning-down BH. This effect shuts off a GRB, and the overall timescale of the GRB could be fitted by the lifetime of the open magnetic flux on the horizon.

Besides the feature of high energy released in very short durations, most GRBs are characterized by highly variable light curves with complex temporal behavior. The usual explanations of the temporal structures range from multiple shock fronts running into the ambient medium (Sari et al. 1996), expanding shells with brighter patches and dimmer regions (Fenimore et al. 1996), to repeated series of pulses with Gaussian or power-law profiles (Norries et al. 1996). However, a clear physical explanation is lacking. Some authors (Fargion & Salis 1996; Blackman et al. 1996; Fargion 1999; Portegies Zwart et al. 1999, hereafter PZLL99; Portegies Zwart & Totani 2001, hereafter PZT01; Fargion & Grossi 2006) suggested that the light curves of GRBs can be explained by a beamed emission from a precessing jet. PZLL99 constructed ad hoc a function $I(t)$ to describe the outline of the light curves, which is characterized by three timescales: a fast rise with timescale $\tau_{\rm rise}$, a plateau phase with timescale $\tau_{\rm plat}$, and a stiff decay with timescale $\tau_{\rm decay}$. The complex temporal structures are modulated by the precession and nutation of the jet. Although their model successfully fits several light curves of GRBs, the origin of the function $I(t)$ is lacking.

In fact, the evolution of the half-opening angle on the BH horizon described in LWM05 provides a natural explanation for the outline of the light curves. Based on LWM05 and PZLL99, in this paper, we intend to combine the evolution of the half-opening angle with the precession and nutation of the jet to fit the complex light curves of GRBs.

The paper is organized as follows. In Sect. 2 we derive the jet luminosity per steradian by the mapping relation between angular coordinate on the BH horizon and the cylindrical radius of the collimated jet. Based on the evolution of an extreme Kerr BH we obtain an intrinsic time variation of the gamma-ray emission. It is shown that the time profile of the emission exhibits a fast rise

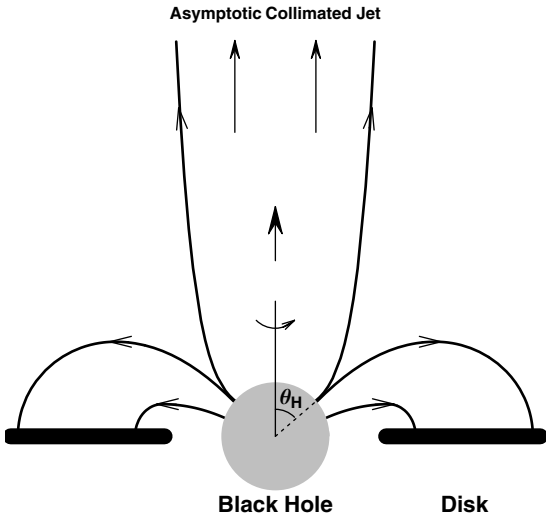

Fig. 1. The polodial topology of the magnetosphere of a disk surrounding a rapidly rotating BH (not to scale). Along the open magnetic flux tube, an asymptotic collimated jet may be formed.

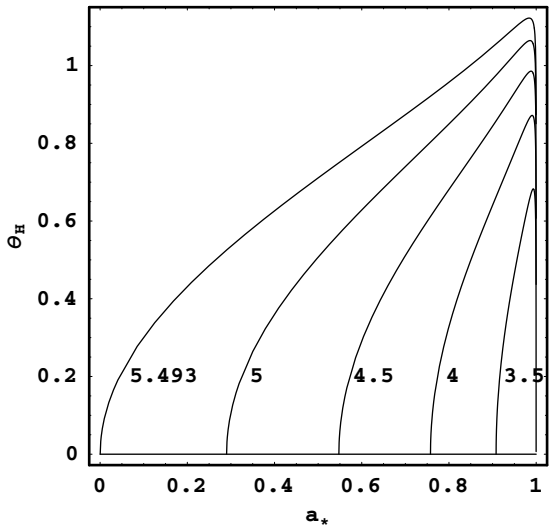

Fig. 2. The curves of $\theta_{\rm H}$ vs. a_* for n = 3.5, 4, 4.5, 5, 5.493.

and a slow decay. In Sect. 3, the light curves of several GRBs are fitted by combining the evolution of the half-opening angle with the precession and nutation of the jet. In Sect. 4, we summarize the main results and discuss some issues related to our model. Throughout this paper the geometry units $G = c = 1$ are used.

2. Time profile of jet luminosity

The poloidal configuration of the magnetic field is shown in Fig. 1, which is adapted from van Putten (2001).

In Fig. 1 the angle $\theta_{\rm H}$ is the half-opening angle of the open magnetic flux tube, indicating the angular boundary between open and closed field lines on the horizon. The angle $\theta_{\rm H}$ can be determined by (Wang et al. 2003)

$$\cos\theta_{\rm H} = \int_1^{\infty} G(a_*;\xi,n)\,{\rm d}\xi. \tag{1}$$

Equation (1) is derived based on the conservation of magnetic flux with three assumptions: (i) the magnetic field on the horizon $B_{\rm H}$ is constant, (ii) the magnetic field on the disk surface $B_{\rm D}$ varies as a power law with the radial coordinate of the disk, and (iii) the magnetic flux connecting the BH with its surrounding disk takes precedence over that connecting the BH to the remote load. In Eq. (1) $a_* \equiv J/M^2$ is the BH spin defined in terms of the BH mass M and the angular momentum J, the parameter n is the power-law index for the variation of $B_{\rm D}$, i.e., $B_{\rm D}^{\infty}\xi^{-n}$, and $\xi \equiv r/r_{\rm ms}$ is the radial coordinate on the disk, which is defined in terms of the radius $r_{\rm ms} \equiv M\chi_{\rm ms}^2$ of the marginally stable orbit (Novikov & Thorne 1973). The function $G(a_*;\xi,n)$ is given by

$$G(a_*;\xi,n) = \frac{\xi^{1-n}\chi_{\rm ms}^2}{2}\sqrt{\frac{1+a_*^2\chi_{\rm ms}^{-4}\xi^{-2}+2a_*^2\chi_{\rm ms}^{-6}\xi^{-3}}{1+a_*^2\chi_{\rm ms}^{-4}+2a_*^2\chi_{\rm ms}^{-6}}} \times\frac{1}{\sqrt{\left(1-2\chi_{\rm ms}^{-2}\xi^{-1}+a_*^2\chi_{\rm ms}^{-4}\xi^{-2}\right)}}. \tag{2}$$

By using Eq. (1) we have the curves of $\theta_{\rm H}$ versus a_* with different values of the power-law index n as shown in Fig. 2, in which the half-opening angle $\theta_{\rm H}$ always increases monotonically with increasing n for a given BH spin a_*.

A very interesting feature shown in Fig. 2 is that the angle $\theta_{\rm H}$ evolves non-monotonically with decreasing a_*, i.e., it increases very rapidly as a_* spins down from unity and then decreases slowly to zero for $3.003 \le n \le 5.493$. Therefore, the time-scale of the duration of the burst is given by the lifetime of rapid spin of the BH as mentioned by van Putten (2001). This evolution characteristic can be applied to fitting GRBs in two aspects: (1) determining the duration of the GRBs as described in LWM05, and (2) shaping the time profile of jet luminosity. To see the latter effect, we will derive the jet luminosity in Sect. 2.1, and investigate its time profile in Sect. 2.2.

2.1. Jet luminosity

As is well known, the rotating energy is extracted from a BH in the form of Poynting flow in the BZ process, and this energy dissipates and accelerates electrons to produce gamma-rays through synchrotron radiation or inverse Compton scattering. Although some works approach the magnetic dissipation in jets, its origin remains unclear (Lyutikov & Blandford 2003; Spruit et al. 2001). As a simple analysis, we introduce a parameter ε_γ to denote the fraction of BZ energy converted into gamma-ray energy.

The BZ power transferred through two adjacent magnetic surfaces between θ and $\theta + {\rm d}\theta$ on the BH horizon is given by (Wang et al. 2002)

$${\rm d}\tilde{P}_{\rm BZ} = {\rm d}P_{\rm BZ}/P_0 = 2a_*^2\frac{k(1-k)\sin^3\theta}{2-(1-q)\sin^2\theta}{\rm d}\theta, \tag{3}$$

where $P_0 \equiv B_{\rm H}^2M^2$, $q \equiv \sqrt{1-a_*^2}$, and k is the ratio of the angular velocity of open magnetic field lines to that of the BH. For the optimal BZ power, $k = 0.5$ is taken.

There are a variety of approaches to studying collimating jet flows, such as the curvature force exerted by the toroidal field (Sakurai 1985), the pressure of the poloidal magnetic field surrounding the jet (Blandford 1993; Spruit 1994), and the pressure of the baryon-rich wind supported by the surrounding disk (van Putten 2001; van Putten & Levinson 2003). The collimation of the flow is determined by the cross-field force-balance in the direction perpendicular to the field. Fendt (1997, hereafter F97) obtained the numerical solution of the stream equation for this force-balance of a force-free magnetic jet. The asymptotic

jet can be collimated into a cylindrical shape with a jet radius of several light cylinder radii.

In order to work out an analytical model we adopt F97's scenario and assume that the poloidal component of the magnetic field of the collimated jet, $B_{\rm L}$, varies as $B_{\rm L}/B_{\rm H} = {\rm e}^{-\lambda x}$, where $x \equiv R/r_{\rm H}$ is the cylindrical radius of the collimated jet in terms of the radius of the BH horizon. Based on the conservation of magnetic flux, we have

$$\Delta\Psi_{\rm H} = B_{\rm H}^2\pi\,(\varpi\rho)_{r=r_{\rm H}}\,{\rm d}\theta = B_{\rm L}^2\pi R{\rm d}R. \quad (4)$$

Substituting $(\varpi\rho)_{r=r_{\rm H}} = \sum_{r=r_{\rm H}}\sin\theta = 2Mr_{\rm H}\sin\theta$ into Eq. (4), we have

$$2\sin\theta\,{\rm d}\theta/(1+q) = x{\rm e}^{-\lambda x}{\rm d}x. \quad (5)$$

Integrating Eq. (5), we obtain the mapping relation between the angular coordinate θ on the BH horizon and the cylindrical radius x the collimated jet as follows

$$\cos\theta = 1 - \frac{1+q}{2\lambda^2}\left[1-(1+\lambda x){\rm e}^{-\lambda x}\right]. \quad (6)$$

Defining $R_{\rm L} \equiv c/\Omega_{\rm F} = 2/\Omega_{\rm H}$ as the light cylindrical radius of the collimated jet, we have $x_{\rm L} \equiv R_{\rm L}/r_{\rm H} = 4/a_*$. Following F97, the radius $R_{\rm jet}$ of a cylindrically collimated jet should be less than $4R_{\rm L}$. In this work, we assume $R_{\rm jet} \approx R_{\rm L}$, and the field lines from $\theta_{\rm H}$ near the BH will connect to $R_{\rm L}$ in the collimated region as shown in Fig. 1. Thus the relation between $\theta_{\rm H}$ and $x_{\rm L}$ is expressed by

$$\cos\theta_{\rm H} = 1 - \frac{1+q}{2\lambda^2}\left[1-(1+\lambda x_{\rm L}){\rm e}^{-\lambda x_{\rm L}}\right]. \quad (7)$$

Following PZLL99, the angle dependence of the jet is given approximately as $x = x_{\rm f}\sin\psi$, where $x_{\rm f} \equiv r_{\rm f}/r_{\rm H}$ is the freezeout distance from the BH to the remote load, where the photons can leave freely. The opening angle $\psi_{\rm jet}$ is fixed by $\sin\psi_{\rm jet} \approx x_{\rm L}/x_{\rm f}$ as PZLL99, and a small opening angle $\psi_{\rm jet} = 6^\circ$ with $x_{\rm f} = 10x_{\rm L}$ is assumed.

Based on the above equations we express the jet luminosity per steradian for an observer at angle ψ with respect to the central locus of the jet, i.e.,

$$\begin{aligned}\tilde{L}_{\rm jet}(a_*,\theta_{\rm H},\psi) \equiv L_{\rm jet}/P_0 &= \varepsilon_\gamma{\rm d}\tilde{P}_{\rm BZ}/{\rm d}\Omega \\ &= \frac{\varepsilon_\gamma{\rm d}\tilde{P}_{\rm BZ}}{2\pi\sin\psi{\rm d}\psi} \\ &= \frac{\varepsilon_\gamma}{2\pi\sin\psi}\frac{{\rm d}\tilde{P}_{\rm BZ}}{{\rm d}\theta}\frac{{\rm d}\theta}{{\rm d}x}\frac{{\rm d}x}{{\rm d}\psi}, \end{aligned} \quad (8)$$

where $\theta_{\rm H} = \theta_{\rm H}(a_*, n)$ is determined by Eq. (1).

Taking $\varepsilon_\gamma \simeq 0.15$ in calculations as given by van Putten et al. (2004), we have $\tilde{L}_{\rm jet}$ varying with ψ as shown in Fig. 3. From Fig. 3 we find that the value of $\tilde{L}_{\rm jet}$ is sensitive to n and a_*. It vanishes at $\psi = 0$, and attains its peak value near the spin axis of the BH. In addition, we find that both the value and the angular coordinate of the peak $\tilde{L}_{\rm jet}$ strongly depend on the values of a_* and n, while the variation of $\tilde{L}_{\rm jet}$ with ψ remains similar.

The $\theta_{\rm H}$ dependence of $\tilde{L}_{\rm jet}$ for the given values of a_* and ψ is depicted in Fig. 4, and we find that the value of $\tilde{L}_{\rm jet}$ is sensitive to that of $\theta_{\rm H}$.

Combining the evolution of $\theta_{\rm H}$ with the BH spin, we have the curves of the luminosity $\tilde{L}_{\rm jet}$ versus a_* as shown in Fig. 5.

Inspecting Fig. 5, we find that the luminosity $\tilde{L}_{\rm jet}$ evolves non-monotonically with the spin of an extreme Kerr BH, increasing very fast at first and then decreasing slowly. This result is understandable by considering the non-monotonic evolution of $\theta_{\rm H}$ with a_* and the monotonic evolution of $L_{\rm jet}$ with $\theta_{\rm H}$ as shown in Figs. 2 and 4, respectively.

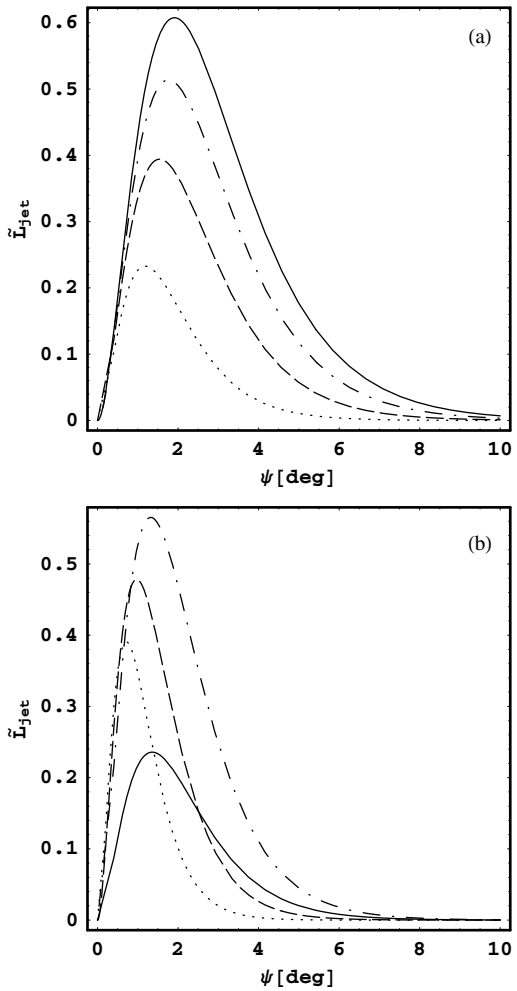

Fig. 3. ψ-dependence of $\tilde{L}_{\rm jet}$ **a)** for $a_* = 0.99$ with $n = 5$, 4.5, 4 and 3.5 in solid, dash-dotted, dashed and dotted lines, respectively, and **b)** for $n = 5$ with $a_* = 0.9999$, 0.9, 0.8 and 0.7 in solid, dash-dotted, dashed and dotted lines, respectively.

2.2. Intrinsic time dependence of jet luminosity

Based on the BH evolution we can derive the time profile of $L_{\rm jet}$. Considering that the angular momentum is transferred from the rapidly rotating BH to the disk, on which a positive torque is exerted, we think that the accretion onto the BH is probably halted. This state is discussed as the suspend accretion state by van Putten & Ostriker (2001), and as the nonaccretion solution by Li (2002). In this state, the BH evolution is governed by the BZ and MC processes. Based on the conservation of energy and angular momentum we have the evolution equations of the BH as follows,

$${\rm d}M/{\rm d}t = -(P_{\rm BZ} + P_{\rm MC}), \quad (9)$$

$$\begin{aligned}{\rm d}a_*/{\rm d}t &= -M^{-2}(T_{\rm BZ}+T_{\rm MC}) + 2M^{-1}a_*(P_{\rm BZ}+P_{\rm MC}) \\ &= B_{\rm H}^2 MA(a_*,n), \end{aligned} \quad (10)$$

and

$$A(a_*,n) \equiv -(T_{\rm BZ}+T_{\rm MC})/T_0 + 2a_*(P_{\rm BZ}+P_{\rm MC})/P_0. \quad (11)$$

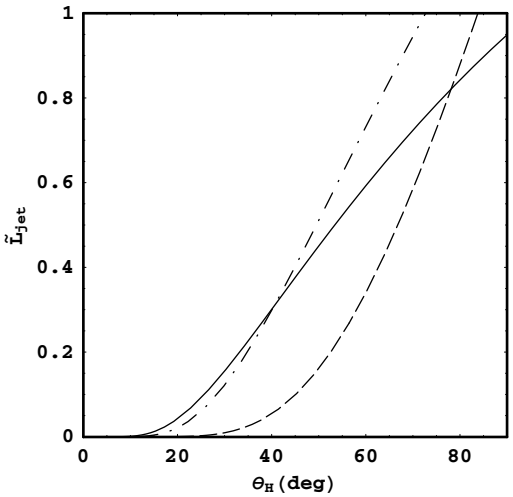

Fig. 4. The curves of $\tilde{L}_{\rm jet}$ vs. $\theta_{\rm H}$ for $a_* = 0.9$ and $\psi = 1^\circ$ (solid line), $a_* = 0.7$ and $\psi = 1^\circ$ (dash-dotted line), and $a_* = 0.9$ and $\psi = 3^\circ$ (dashed line).

The powers and torques for the BZ and MC processes are expressed as (Wang et al. 2003),

$$\tilde{P}_{\rm BZ} \equiv P_{\rm BZ}/P_0 = 2a_*^2 \int_0^{\theta_{\rm H}} \frac{k(1-k)\sin^3\theta\,{\rm d}\theta}{2-(1-q)\sin^2\theta} \tag{12}$$

$$\tilde{T}_{\rm BZ} \equiv T_{\rm BZ}\Big/T_0 = 4a_*(1+q) \int_0^{\theta_{\rm H}} \frac{(1-k)\sin^3\theta\,{\rm d}\theta}{2-(1-q)\sin^2\theta} \tag{13}$$

$$\tilde{P}_{\rm MC} \equiv P_{\rm MC}\Big/P_0 = 2a_*^2 \int_{\theta_{\rm H}}^{\pi/2} \frac{\beta(1-\beta)\sin^3\theta\,{\rm d}\theta}{2-(1-q)\sin^2\theta} \tag{14}$$

$$\tilde{T}_{\rm MC} \equiv T_{\rm MC}\Big/T_0 = 4a_*(1+q) \int_{\theta_{\rm H}}^{\pi/2} \frac{(1-\beta)\sin^3\theta\,{\rm d}\theta}{2-(1-q)\sin^2\theta} \tag{15}$$

where $T_0 \equiv B_{\rm H}^2 M^3$, and $\beta \equiv \Omega_{\rm D}/\Omega_{\rm H}$ is the ratio of the angular velocity of the disk to that of the BH.

Substituting Eqs. (9) and (10) into Eq. (8), we have the curves of $L_{\rm jet}(t)$ varying with time t for different values of ψ and n as shown in Fig. 6. The magnetic field on the BH horizon $B_{\rm H} = 10^{15}G$, the initial BH mass $M(0) = 7\ M_\odot$ and the initial BH spin $a_*(0) = 1$ are assumed in calculations.

As shown in Fig. 6, the time profiles of $L_{\rm jet}$ exhibit a feature of fast-rise and slow-decay, which arises from the non-monotonic evolution characteristic of $\theta_{\rm H}$ in terms of the BH spin as shown in Fig. 2. Thus the intrinsic time profile of the jet luminosity is derived naturally in our model rather than assumed ad hoc, and it resembles that given in PZLL99. The shapes of the profiles can be adjusted by changing the values of n and ψ. It has been argued in LWM05 that the durations of various GRBs can be fitted by changing the value of n for the given initial BH spin.

3. Fitting observed light curves

3.1. Precessing jet

The misalignment in the spin axis of the BH and the angular momentum axis of the binary causes the accretion disk around the BH to precess, which is known as the slaved disk precession. PZLL99 investigated the precession of the accretion disk in the gamma-ray binary, in which a neutron star fills its Roche lobe

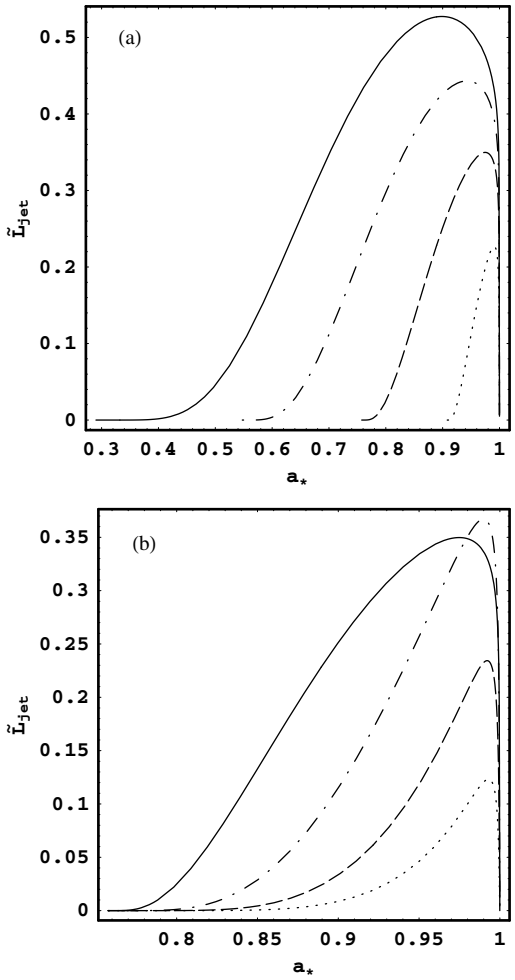

Fig. 5. The curves of $\tilde{L}_{\rm jet}$ vs. a_* **a)** for $\psi = 1^\circ$ with $n = 5$, 4.5, 4 and 3.5 in solid, dash-dotted, dashed and dotted lines, respectively; **b)** for $n = 4$ with $\psi = 1^\circ$, 2°, 3° and 4° in solid, dash-dotted, dashed and dotted lines, respectively.

and transfers its mass to a BH. It is shown that this system has a precession period of about a second. The Lense-Thirring precession appears for a Kerr BH, if the accretion disk is inclined with respect to the equatorial plane of the BH (Lense & Thirring 1918). Recently, Reynoso et al. (2006, hereafter RRS06) studied the possible effect of Lense-Thirring precession on neutrino-cooled accretion disks. It is found that the precession period can be much less than 1 s.

As the magnetic field is assumed to be anchored in the disk, this would result in the jet perpendicular to the midplane of the disk, and the precession and nutation of the disk directly implies the precession and nutation of the jet. To describe the jet kinematically we adopt the angular evolution of the jet in terms of the spherical angles $\theta_{\rm jet}$ and $\phi_{\rm jet}$ given in PZLL99 as follows,

$$\phi_{\rm jet} = \Omega_{\rm pre}(t - t_0) + \frac{\Omega_{\rm pre}}{\Omega_{\rm nu}} \sin(\Omega_{\rm nu} t), \tag{16}$$

$$\theta_{\rm jet} = \theta_{\rm jet}^0 + \frac{\Omega_{\rm pre}}{\Omega_{\rm nu}} \tan\theta_{\rm jet}^0 \cos(\Omega_{\rm nu} t), \tag{17}$$

where $\Omega_{\rm pre} = 2\pi/\tau_{\rm pre}$ and $\Omega_{\rm nu} = \pm 2\pi/\tau_{\rm nu}$ are the angular frequencies of precession and nutation with periods $\tau_{\rm pre}$ and $\tau_{\rm nu}$, respectively. The direction of the observer can be assigned as $\theta_{\rm obs}$ and $\phi_{\rm obs}$. A schematic picture of the precessing disk and jet is

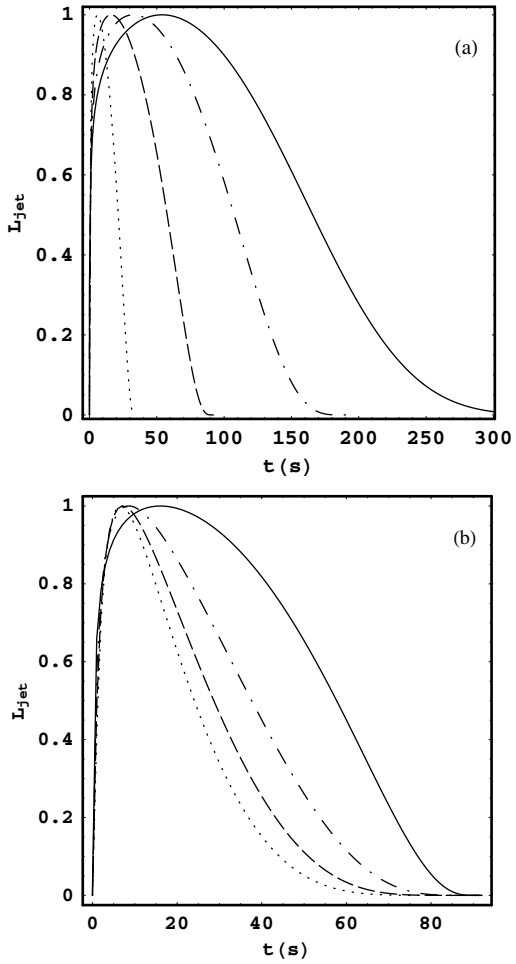

Fig. 6. The curves of $L_{\rm jet}$ vs. time t for different n and observed angle ψ, each curve is normalized to unity at its maximum: **a)** for $\psi = 1^\circ$ with $n = 5$, 4.5, 4 and 3.5 in solid, dash-dotted, dashed and dotted lines, respectively; **b)** for $n = 4$ with $\psi = 1^\circ$, 2°, 3° and 4° in solid, dash-dotted, dashed and dotted lines, respectively.

Table 1. Free parameters that may vary per burst.

Parameters	Note
n	The power-law index for the variation of the magnetic field on the disc
$\tau_{\rm pre}$	Precession period
$R_\Omega \equiv \Omega_{\rm nu}/\Omega_{\rm pre}$	Frequency ratio of nutation to precession
$\theta^0_{\rm jet}$	Initial angular coordinate of a jet
$\theta_{\rm obs}, \phi_{\rm obs}$	Observation angles

shown in Fig. 7, and the angle between the observer and the central locus of the jet is

$$\psi = \cos^{-1}(\hat{r}_{\rm obs} \cdot \hat{r}_{\rm jet}). \quad (18)$$

3.2. Fittings

Substituting Eq. (18) into Eq. (8), we obtain the gamma-ray luminosity of a prcessing jet $L_{\rm jet}(t)$, which is adopted to fit the observed complex light curves of GRBs. The model contains six free parameters to fit the light curves (as described in Table 1), and the fitting procedures are described as follows.

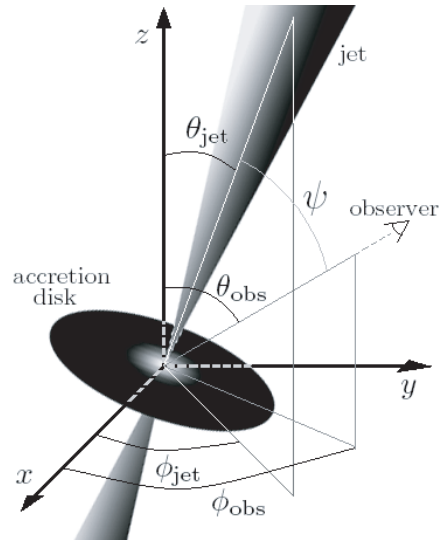

Fig. 7. A schematic picture of a precessing disk with jet (adapted from RRS06).

The first step is to determine the background. Following PZLL99, this is done by averaging the count rate of the initial, ∼1800 data. The background is subtracted in our fitting process.

Next, we introduce the start time $\tau_{\rm start}$ and the end time $\tau_{\rm end}$, which are the times of the start-up and shut-off of the real burst, respectively. As a rough estimate, we take $\tau_{\rm start}$ and $\tau_{\rm end}$ as the first and last time to reach about 1% of the peak count rate. Our model fits the light curve from $\tau_{\rm start}$ to $\tau_{\rm end}$.

From Figs. 2 and 6a, we find that the duration of GRB is sensitive to the value of n. Therefore, the first free parameter n is chosen to satisfy the observed duration ($\tau_{\rm end} - \tau_{\rm start}$) in our model. Substituting n into Eqs. (10) and (11), we obtain the evolution functions of BH mass $M(t)$, BH spin $a_*(t)$ and half-opening angle $\theta_{\rm H}(t)$. The precessing effect is described by the function $\psi(t)$. Substituting these functions into Eq. (8), we can produce the time variability of the observed flux.

Finally, we use the simulated annealing to fit the observed bursts. The other five parameters in Table 1, i.e., $\tau_{\rm pre}$, R_Ω, $\theta^0_{\rm jet}$, $\theta_{\rm obs}$ and $\phi_{\rm obs}$ are chosen freely in this simulation. After each iteration we determine the χ^2 from the fitting of $L_{\rm jet}(t)$ to the observed burst profile. This value is minimized by the annealing algorithm.

We apply this model to fit several observed GRBs by adjusting the value of the above six free parameters (see Table 1). The data of the light curves are taken from BATSE and HETE. We fit the light curves of GRBs from the third energy channel, i.e., 100−300 keV for BATSE, and 30−400 keV for HETE. The fittings results are presented in Fig. 8 with the parameters listed in Table 2.

Inspecting Fig. 8, we find that the light curves of these GRBs can be fitted by our model. Some simple light curves of GRBs are fitted in a rather satisfactory way as shown in Figs. 8a, c, e, g, and complicated light curves are fitted with good overall shapes as shown in Figs. 8b and 8d. Figure 8f shows the fitting for the more complicated burst GRB 030519a for which most of the peaks are well fitted except for the third one. GRB 920701 is a peculiar asymmetric burst (Romero et al. 1999; RRS06), with a slower rise and a faster decay compared with the other bursts. It turns out that this type of burst can be also fitted by our model as shown in Fig. 8b.

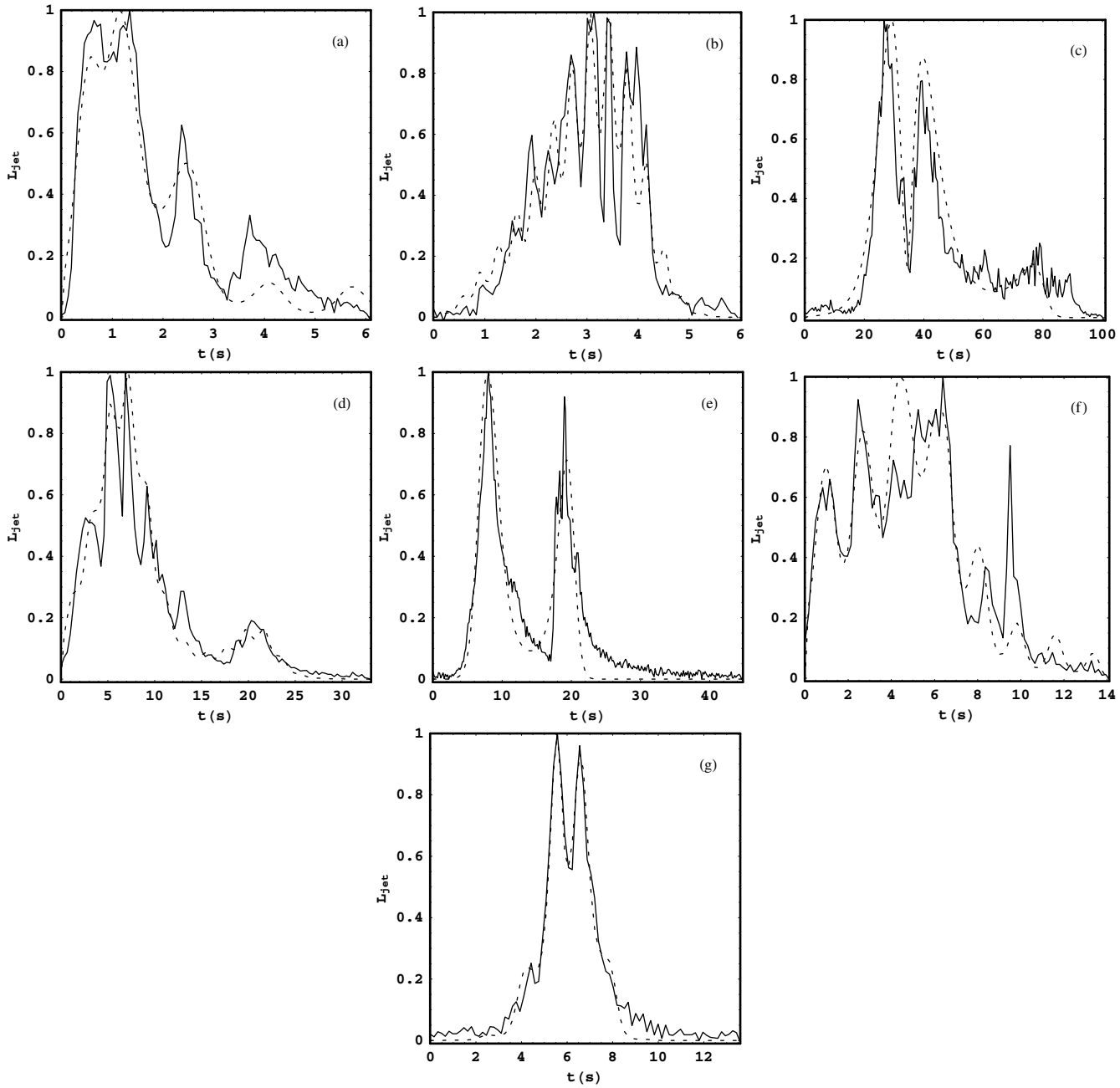

Fig. 8. Fits of the light curves from the third energy channel of **a)** GRB 910717; **b)** GRB 920701; **c)** GRB 990123; **d)** GRB 001225; **e)** GRB 030329; **f)** GRB 030519a and **g)** GRB 031111a. The real bursts profile and the fitting curves are plotted in full and broken curves, respectively.

Table 2. Values of the parameters for fitting several GRBs.

GRB	$\tau_{\rm start}$ (s)	$\tau_{\rm end}$ (s)	n	$\tau_{\rm pre}$ (s)	R_Ω	$\theta^0_{\rm jet}$ (deg)	$\theta_{\rm obs}$ (deg)	$\phi_{\rm obs}$ (deg)	χ^2
910717	1.86	7.94	3.15	7.00	4.22	1.78	0.89	39.16	0.88
920701	1.02	6.98	3.10	7.24	20.01	2.63	0.69	188.25	1.52
990123	0.51	100.86	4.10	128.37	1.11	3.89	2.97	149.17	2.05
001225	0.28	33.37	3.60	14.68	6.08	0.74	4.28	172.58	0.84
030329	7.24	51.99	3.70	70.89	2.60	11.16	11.20	69.88	1.78
030519a	0.09	14.18	3.26	7.80	4.35	1.54	0.41	259.86	1.63
031111a	2.56	16.16	3.26	22.13	12.86	5.58	4.96	101.63	0.14

4. Discussion

In this paper we discuss a model for fitting the light curves of GRBs based on the coexistence of the BZ and MC processes, combining the evolution of an extreme Kerr BH surrounded by a precessing disk. Comparing with PZLL99 , PZT01 and RRS06, our model can explain both the intrinsic time profile and the observed duration of GRB. The fittings are done with only six parameters. However, there are still several issues related to this model and the fittings.

First, a precessing jet tends to produce light curves in which subsequent peaks appear at periodic intervals. However, the observed gamma-ray bursts show no evidence for periodicities at any time-scale. PZT01 solved this problem by considering the interaction between the jet and the interstellar medium. In our model, the distance from the BH to the emission region is fixed. If this distance varies during the GRB, the asymmetry of the subsequent peaks in the light curves could be explained by our model.

Second, the individual peaks produced by precession clearly lack the observed strong asymmetries, i.e., a fast rise and a slow decay (Fenimore et al. 1996). In our model, the time variability of the central engine is rather smooth. Thus our model cannot explain the strong asymmetries. As described in PZT01, the effect of the curvature of the jet front or the cooling of gamma-ray emitting electrons can make the pulse profile a "fast rise and slow decay". We will take these effects into account in future work.

Third, this model is good in fitting the overall shapes of the light curves of the bursts, but it is difficult to fit the smaller details such as the variability on time scales of milliseconds. Recently, Wang et al. (2006) discussed the modulations of the screw instability in the BZ process on the light curves of GRBs, and they argued that the variability timescales of ten milliseconds can be interpreted by two successive flares due to the screw instability of the magnetic field. It is also shown that the individual peaks produced by releasing and recovering magnetic energy have a fast rise and slow decay profile. We shall improve the fitting of the light curves of GRBs by combining the jet precession with screw instability of the magnetic field in future work.

We cannot perform satisfactory fits for all kinds of GRB light curves with this simple model, especially for those displaying extraordinary periods of quiescence between bursts. Figure 8f is one of these cases, where a time-lag in the third peak is not reproduced. This type of burst is hard to fit by the jet-time-profile as given in Fig. 6, i.e., the feature of fast-rise and slow-decay. The combinations of parameters listed in Table 2 are not unique in the fittings. For example, the light curve of GRB 920701 can be fitted as well as Fig. 8b with the parameters ($n = 3.10$; $\tau_{\rm pre} = 5.18$, $R_\Omega = 8.36$; $\theta^0_{\rm jet} = 1.02$, $\theta_{\rm obs} = 1.19$, $\phi_{\rm obs} = 242.58$).

Acknowledgements. We thank the anonymous referee for numerous constructive suggestions. This work is supported by the National Natural Science Foundation of China under Grant Numbers 10573006 and 10121503. This research has made use of the HETE and BATSE data.

References

Blackman, E. G., Yi, I., & Field, G. B. 1996, ApJ, 473, L79
Blandford, R. D. 1993, in Astrophysical Jets, ed. D. Burgarella, M. Livio, & C. O'Dea (Cambridge: Cambridge University Press), 15
Blandford, R. D. 1999, in Astrophysical Discs: An EC Summer School, ed. J. A. Sellwood, & J. Goodman (San Francisco: ASP), ASP Conf. Ser., 160, 265
Blandford, R. D., & Znajek, R. L. 1977, MNRAS, 179, 433
Bloom, J. S., Kulkarni, S. R., Djorgovski, S. G., et al. 1999, Nature, 401, 453
Brown, G. E., Lee, C.-H., Wijers, R. A. M. J., et al. 2000, NewA, 5, 191
Camenzind, M. 1987, A&A, 184, 341
Fargion, D. 1999, A&AS, 138, 507
Fargion, D., & Salis, A. 1996 [arXiv:astro-ph/9605166]
Fargion, D., & Grossi, M. 2006, ChJAA, 6S1, 342
Fendt, C. 1997, A&A, 319, 1025 (F97)
Fenimore, E. E., Madras, C. D., & Nayakshin, S. 1996, ApJ, 473, 998
Galama, T. J., Vreeswijk, P. M., van Paradijs, J., et al. 1998, Nature, 395, 670
Lee, H. K., Wijers, R. A. M. J., & Brown, G. E. 2000, Phys. Rep., 325, 83
Lei, W. H., Wang, D. X., & Ma, R. Y. 2005, ApJ, 619, 420 (LWM05)
Lense, J., & Thirring, H. 1918, Phys. Z., 19, 156
Li, L. X. 2000, ApJ, 533, L115
Li, L. X. 2002, ApJ, 567, 463
Lovelace, R. V. E., Berk, H. L., & Contopoulos, J. 1991, ApJ, 379, 696
Lyutikov, M., & Blandford R. 2003 [arXiv:astro-ph/0312347]
MacDonald, D., & Thorne, K. S. 1982, MNRAS, 198, 345
MacFadyen, A. I., & Woosley, S. E. 1999, ApJ, 524, 262
Norris, J. P., Nemiroff, R. J., Bonnell, J. T., et al. 1996, ApJ, 459, 393
Novikov, I. D., & Thorne, K. S. 1973, in Black Holes, ed. C. Dewitt (New York: Gordon and Breach), 345
Paczynski, B. 1986, ApJ, 308, L43
Piran, T. 2004, Rev. Mod. Phys., 76, 1143
Portegies Zwart, S. F., & Totani, T. 2001, ApJ, 328, 951 (PZT01)
Portegies Zwart, S. F., Lee, C. H., & Lee, H. K. 1999, ApJ, 529, 666 (PZLL99)
Reynoso, M. M., Romero, G. E., & Sampayo, O. A. 2006, A&A, 454, 11 [arXiv:astro-ph/0511639] (RRS06)
Romero, G. E., Torres, D. F., Andruchow, I., & Anchordoqui, L. A. 1999, MNRAS, 308, 799
Sakurai, T. 1985, A&A, 152, 121
Sari, R., Narayan, R., & Piran, T. 1996, ApJ, 473, 204
Spruit, H. C. 1994, in Cosmical Magnetism, ed. D. Lynden-Bell (Dordrecht: Kluwer), 33
Spruit, H. C., Daigne, F., & Drenkhahn, G. 2001, A&A, 369, 694
Wang, D. X., Xiao, K., & Lei, W. H. 2002, MNRAS, 335, 655
Wang, D. X., Ma, R. Y., Lei, W. H., & Yao, G. Z. 2003, ApJ, 595, 109
Wang, D. X., Lei, W. H., & Ye, Y. C. 2006, ApJ, 643, 1047
Woosley, S. E. 1993, ApJ, 405, 273
van Putten, M. H. P. M. 1999, Science, 284, 115
van Putten, M. H. P. M. 2001, Phys. Rep., 345, 1
van Putten, M. H. P. M., & Ostriker, E. C. 2001, ApJ, 552, L31
van Putten, M. H. P. M., & Levinson, A. 2003, ApJ, 584, 937
van Putten, M. H. P. M., Levinson, A., Regimbau, T., Punturo, M., & Harry, G. M. 2004, Phys. Rev. D, 69, 044007